Hindawi
Journal of Nanomaterials
Volume 2022, Article ID 1408529, 18 pages
https://doi.org/10.1155/2022/1408529

Research Article

Inconel 718 Turning Process Parameters Optimization with MQL Nanofluid Based on CuO Nanoparticles

Pravin A. Mane,[1] **Anupama N. Kallol**,[2] **Rajendra L. Doiphode**,[3] **G. A. Manjunath**,[2] **Bahaa Saleh**,[4] **Mohamed Abbas**,[5,6] **C. Ahamed Saleel**,[7] **and Ibrahim M. Alarifi**[8]

[1]*Gogte Institute of Technology, Belagavi, Karnataka, India*
[2]*Department of Mechanical Engineering, Gogte Institute of Technology, Belagavi, India*
[3]*Department of Mechanical Engineering, Government Polytechnic, Kolhapur, India*
[4]*Mechanical Engineering Department, College of Engineering, Taif University, P.O. Box 11099, Taif 21944, Saudi Arabia*
[5]*Electrical Engineering Department, College of Engineering, King Khalid University, Abha 61421, Saudi Arabia*
[6]*Computers and Communications Department, College of Engineering, Delta University for Science and Technology, Gamasa 35712, Egypt*
[7]*Department of Mechanical Engineering, College of Engineering, King Khalid University, PO Box 394, Abha 61421, Saudi Arabia*
[8]*Department of Mechanical and Industrial Engineering, College of Engineering, Majmaah University, Al-Majmaah, Riyadh 11952, Saudi Arabia*

Correspondence should be addressed to Pravin A. Mane; pravin2015@gmail.com and Ibrahim M. Alarifi; i.alarifi@mu.edu.sa

Received 15 March 2022; Accepted 9 August 2022; Published 19 September 2022

Academic Editor: Omer Alawi

This study examined the effects of a minimum quantity lubrication (MQL) and a Cupric oxide- (CuO-) based nanofluid on Inconel 718 machinability. Additionally, by using an MQL CuO-based nanofluid during the turning process, Inconel 718's tribological characteristics are optimised. The experimentation was done using the minimum quantity lubrication (MQL) method. With the aid of magnetic stirring and an ultrasonic bath process, CuO nanoparticles were dispersed in distilled water, sunflower oil, and soyabean oil to create nanofluid. Soyabean oil contains uniformly distributed CuO nanoparticles. All the experimental trials are designed based on the L_{18} Taguchi-based orthogonal arrays and performed on CNC turning under MQL and nanofluid environment. There are four input parameters that were selected at mixed level, namely, cutting speed, feed rate, weight % of CuO in the nanofluid, and flow rate to analyze surface roughness and tool wear. In addition to that, the response surface method was used to identify the optimum condition for better surface roughness and tool wear. Surface roughness and tool wear were measured using the surface roughness tester and toolmaker's microscope, respectively. Experimental results observed that cutting speed and weight % highly affect surface roughness whereas cutting speed and flow rate affect tool wear. The predicted optimal values for lower surface roughness are 160 ml/hr flow rate, 92.99 m/min cutting speed, 3 weight % of CuO, and 0.1 mm/min feed rate and for low tool wear 80 ml/hr flow rate, 92.99 m/min cutting speed, 3 weight % of CuO, and 0.1 mm/min feed rate.

1. Introduction

Inconel 718 is broadly applied in the aerospace, marine, steam turbine, power plants, nuclear reactors, pumps, and aircraft engine industries due to its ability to maintain strength in high-temperature environments. Close dimensional tolerance and high level of surface polish have become essential machining parameters for their application. Among that, surface quality is a critical parameter when machining Inconel 718. Researchers and tribologists are looking into coated tools, cryogenic cooling, MQL, synthetic lubricants, micro- and nanosolid lubricants, vegetable oil-based lubricants, and nanofluids to produce an excellent machined surface. Cooling, water vapour cooling, solid lubricants, and

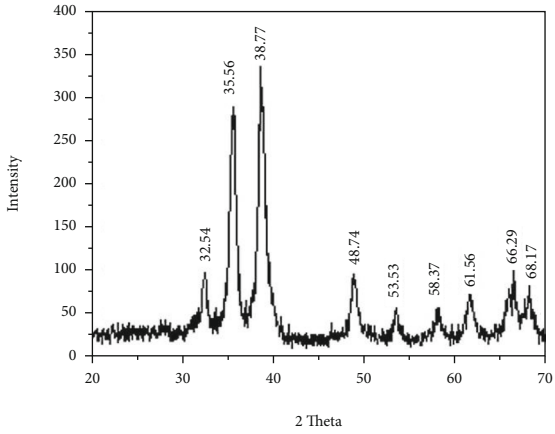

Figure 1: X-ray diffraction pattern of CuO nanoparticles.

minimum quantity lubrication (MQL) are the alternatives to flood cooling. As a result, researchers worldwide have tried and proposed using a small amount of lubricant in the industry. With the decrease on the impact of flood cooling on workers' health, MQL technique had the edge over flood cooling. MQL is proving as a promising method to improve the performance of the machining process. Therefore, the MQL system is environmentally friendly and it also improves the machinability [1, 2]. This MQL system has edge if it is used with nanofluid and gives better results than only MQL [3]. Effectiveness of MQL with nanofluid has resulted into better tribological properties in cutting zone with vegetable oil [4].

When it comes to cutting difficult-to-machine metals like Inconel and titanium, MQL is an effective replacement for flood cooling. So, to give an edge to MQL while machining these materials, MQL is assisted with nanolubricants to improve performance. The novelty of base fluid having nanoparticles can be enhanced by using an MQL system that can be dispersed in the mist form [5, 6]. From economic, environmental, and technical points of view, nanofluids are the first choice among all other lubrication techniques. From a lubrication point of view, nanofluid with the MQL system and the cryogenic system is the best option [7]. To improve the efficiency of nanoparticles in base fluid, basically three factors such as thermal conductivity, stability, and viscosity are important [8].

As base fluid enriches with nanoparticles, the number of nanoparticles at the tool-workpiece interface increases. These results decrease in contact between workpiece and tool by acting as a spacer between tool and workpiece; consequently, surface roughness is reduced [9–11]. Increasing nanoparticles' concentration, surface roughness firstly decreased then it increased because of the agglomeration at a high concentration which lowers the efficiency of nanofluid by transferring contact region from line to surface [12, 13]. Hegab and Kishawy investigated the effectiveness of different nanoparticles by utilizing the same volume fraction of nanofluids and discovered that using nanoparticles increased machining performance with cutting materials that are tough to cut, such as Inconel 718 [9]. Venkatesan et al. used Al_2O_3 nanofluid in olive oil to enhance turning process parameters for Inconel X-750. They discovered that tool wear and force rise as the % concentration of nanoparticles increases up to 0.5%, after which they begin to fall [14].

Feed rate and nanoparticle concentration have the highest impact on surface roughness [15–18]. Amrita et.al varied flow rate of mist application working environment having speed, depth of cut, and constant feed while machining AISI 1040 steel. They discovered a high concentration of nanofluids with less flow rate has the same result for tool-chip interface temperature as that of flood cooling, but it decreases with an increase in concentration and flow rate and hence leading to less tool wear [19]. Vazquez et al. studied tool life in machining process using CuO-based nanofluid. The tool's service life was improved by 604% by applying CuO nanofluid. CuO nanoparticles possess antiwear behaviour. This is due to the rolling action and CuO deposition on worn surfaces, which results in a lower frictional coefficient [20].

Using Al_2O_3 as a nanofluid, Mani et al. adjusted cutting settings and particle concentration during turning of EN8. The process parameters employed to measure surface roughness were the depth of cut, nanoparticle concentration, feed, and speed. Major affecting factors on roughness were discovered to be nanoparticle concentration and feed using ANOVA [21]. Prasad et al. used MQL to test the incorporation of graphite nanoparticles in cutting fluid during AISI 1040 turning. Graphite nanoparticles were used in 0, 0.1, 0.3, and 0.5 weight % concentrations in cutting fluid with MQL technique having 15 ml/hr and 5 ml/hr flow rate. Surface roughness was decreased with the inclusion of graphite nanoparticles and found a minimum of 0.3 weight % inclusion of nanoparticles for 15 ml/hr flow rate [22]. In the same content, Usha and Rao found that MQL depth of cut, cutting speed, and flow rate are primary important factors on influencing roughness [23]. Thakur et al. tested SiC nanoparticles for EN-24 material with 0.5, 1, and 1.5 weight % and found 1.5 weight % SiC nanofluid to show minimum surface roughness. This may be due to 0.5 weight % SiC nanofluid having the lowest coefficient of friction and greatest thermal conductivity leading to the cooling effect, and hence less surface roughness and tool wear were obtained [24].

Speed, percentage of nanoparticles, feed rates, and nozzle angles, each of three levels, were selected to analyze tool wear, surface roughness, and power usage. They found that the feed rate greatly influences roughness, whereas a high percentage of particles contribute to reduced tool wear, increasing feed rate [25]. Researchers start taking benefits of nanolubricants and conventional process factors like feed, speed, and depth of cut along SiO2 percentage to analyze cutting temperature and roughness [26].Cutting speed, feed, and percentage concentration of nanoparticles are also used as process parameters by the researchers to measure tool flank wear, roughness, cutting force, temperature, and energy consumption. They found that nanoparticles' concentration is the most affecting factor for all responses [27–29].

The effect of MQL and nano-MQL environment in face turning of Inconel 800 was studied by Ramanan et al.

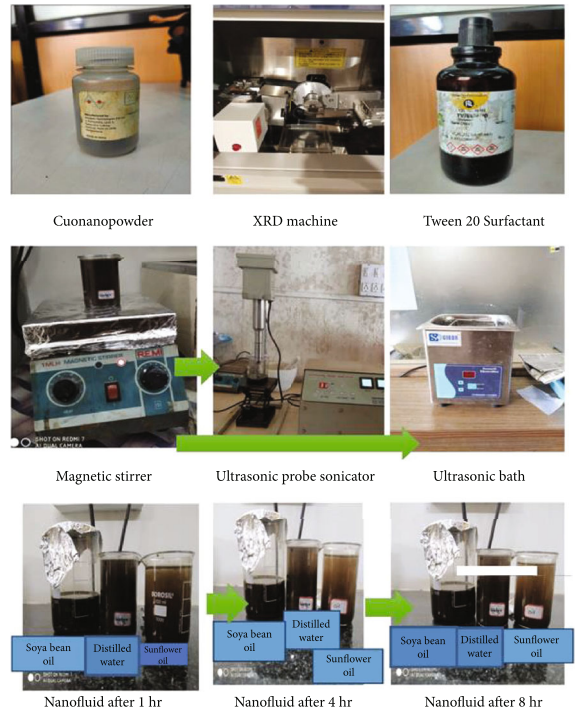

Figure 2: Preparation of nanofluid.

Figure 3: Cleveland flashpoint and fire point apparatus.

Table 1: Smoke point, flash point, and fire point.

Sr. no.	Soyabean oil	Reading in °C
1	Smoke point	299
2	Flash point	335
3	Fire point	350

Minimum abrasion and crater wear were seen in nano-MQL as compared to other cooling techniques, also high concentration of nanoparticle enhanced the tool life [30]. Similarly, the effect of MQL and nano-MQL in the machining of ER 7 steel was studied by Camali et al. Experimental results observed that the usage of MQL in the machining surface roughness and tool life was improved as compared to the dry cutting condition. Further, this machining performance is enhanced by using nanoparticles [31]. Influence of duplex jet cooling system on machining performance of Nimonic

Figure 4: Redwood viscometer.

Table 2: Kinematic viscosity of base oil.

Sr. no	Temp. of water ˚C	Temp. of oil ˚C	Time (sec)	Kinematic viscosity (poise)
1	25	25	189	0.4641
2	43	42	107	0.2596
3	63	61	66	0.1640
4	76	74	53	0.1283
5	89	87	48	0.1143

Table 3: Kinematic viscosity of nanofluid.

Sr. no	Temp. of water ˚C	Temp. of oil ˚C	Time (sec)	Kinematic viscosity (poise)
1	25	25	210	0.5163
2	43	41	147	0.3596
3	63	60	102	0.2470
4	76	74	83	0.2097
5	89	86	66	0.1640

80A was analysed by Korkmaz et al. They observed that the usage of nanofluid enhanced the machine surface roughness quality. Further, they correlate the surface roughness with types of chips that were formed during the machining [32].

Based on the above cited literature, it is noticed that limited study is available to find out the effect of weight % of CuO nanoparticles with their flow rate using the MQL on the turning process of lnconel 718. Further, while conventionally turning, most of the researchers used cutting speed, feed, and depth of cut as process parameters. Very few researchers considered the flow rate of the MQL system as a process parameter and its effect on the output parameters. At the same time it is also observed that CuO nanofluid is proving better heat-carrying nanofluid than any other nanofluid. So its effect during machining of difficult-to-cut material like Inconel 718 needs to be studied by considering CuO nanoparticles' weight % and its low rate as a process parameter.

Hence, in this study 18 experiments were carried out on Inconel 718 superalloy workpiece which focuses on the tribological properties in terms of (i) optimization of surface roughness for Inconel 718 turning process parameters with MQL nanofluid, (ii) optimization of tool wear for Inconel 718 turning process parameters with MQL nanofluid, and (iii) determining the influencing factors on tribological properties of Inconel 718 during turning process with MQL nanofluid.

This work focuses on optimizing turning process parameters like speed, feed, nanoparticles' weight %, and flow rate of Inconel 718 using MQL.

2. Material and Methods

CuO nanoparticles are selected in the present research study because of it having a highest thermal conductivity among all metals and it can carry more heat efficiently than any other metal. CuO nanoparticles were purchased from Amnium Technology Pvt. Ltd. Pune. The size of this purchased nanopowder was measured on the XRD machine at D.Y. Patil Medical, deemed university, Kolhapur.

(i) XRD machine was utilised to measure nanoparticle size. The 2 theta graphs obtained from XRD machine is shown in Figure 1

From which, it is clear that the maximum value of 2 thetas is 38.77. This value size of nanoparticles was

(a)

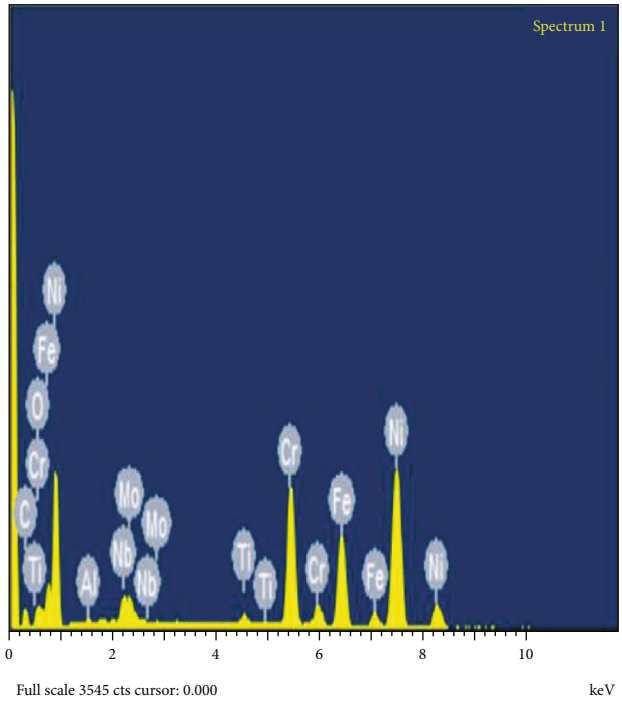

(b)

Figure 5: (a) SEM and (b) EDM spectrum of Inconel 718 material.

Table 4: Chemical composition of Inconel 718.

Element	C	O	Al	Ti	Cr	Fe	Ni	Nb	Mb
Weight %	12.07	2.06	0.40	0.68	17.30	16.15	45.34	3.77	2.22

Table 5: CNC machine specification.

Machine name:	CNC turning Centre
Manufacturer	Laxmi machine work ltd.
Technical specifications	
Chuck diameter	210 mm max
Maximum turning Centre	320 mm max
Bar capacity	40 mm max
Maximum machining diameter	160 mm
Spindle speed range	3000-3500 rpm
Feed range in mm/min	1 to 2000
Turret - no. of station	8 nos.

Table 6: Controlled parameters.

Sr. no.	Controlled parameters
1.	Cutting speed (m/min)
2.	Feed (mm/min)
3.	Weight % of CuO
4.	Flow rate (ml/hr.)

Table 7: Constant parameters.

Sr. no.	Constant parameters	
1.	Cutting fluid	CuO nanolubricant
2.	Work material	Inconel 718
3.	Tool insert	TiAlN coated carbide
4.	Depth of cut	1 mm

Table 8: Taguchi based orthogonal array.

Expt. no	Flow rate	Cutting speed	Weight %	Feed rate
1	80	92.99	1	0.1
2	80	92.99	2	0.2
3	80	92.99	3	0.3
4	80	104.61	1	0.1
5	80	104.61	2	0.2
6	80	104.61	3	0.3
7	80	116.23	1	0.1
8	80	116.23	2	0.2
9	80	116.23	3	0.3
10	160	92.99	1	0.1
11	160	92.99	2	0.2
12	160	92.99	3	0.3
13	160	104.61	1	0.1
14	160	104.61	2	0.2
15	160	104.61	3	0.3
16	160	116.23	1	0.1
17	160	116.23	2	0.2
18	160	116.23	3	0.3

calculated by the Debye-Scherrer equation.

$$\text{Crystallite size } (D) = \frac{0.9A}{B \cos C}, \quad (1)$$

where A = X-ray source wavelength = 1.5406. B = Half maximum diffraction width at full width. C = Angle (Bragg angle of an intense peak). $2C$ = 38.77. So, C = 19.43. B = 0.0177. Therefore, D = 0.9 ∗ 1.5406 ∗ 10^ (-10)/0.0177 ∗ cos (19.43). D = 8.39 Nm.

2.1. Preparation of Nanofluid. The basic step towards this research is to prepare CuO-based nanofluid. Specifications of the XRD machine are Model-Rigaku Miniflex - 600 (Japan), maximum power - 600 watts, tube voltage - 40 kV, tube current - 15 mA, scanning range - 3 to 145° (2⊠), scanning speed - 0.01 to 100° (minimum 2Θ), min. step width - 0.005° (2Θ), and accuracy - ± 0.02°.

The literature found that vegetable oil was selected by most of the researchers as the base fluid for CuO nanoparticles. Hence, sunflower oil and distilled water were selected as fluids for the dispersion of CuO nanoparticles. But nanoparticles agglomerate in sunflower oil and distilled water. Hence, finally, soyabean oil was selected as base fluid. Sodium dodecylbenzene sulfonate as a surfactant was added to the base fluid for better stability of nanoparticles in the base fluid.

Initially, a magnetic stirrer for a continuous 8 hr was used for mixing nanoparticles in the base fluid. But after 1 hr of magnetic stirrer, CuO nanoparticles start to agglomerate at the bottom of the base fluid. Then, for uniform distribution and stabilization of nanoparticles, magnetic stirrer followed by an ultrasonic probe was used. It was found that after 4 hr, nanoparticles start agglomerating. Hence, magnetic stirrer for 3 hr followed by an ultrasonication bath process for 2 hr was used to uniformly distribute and stabilize CuO nanoparticles [33–36]. The procedure followed in the preparation of nanofluid is well illustrated in Figure 2.

2.2. Specifications of Magnetic Stirrer

(i) Maximum speed-1200 rpm including step-less variable speed and decent speed steadiness, heating capacity - 600 W, hotplate size - 175 mm dia, acid, and alkali resistive, supply – 220/240 V,50 Hz, AC, and top plate material – stainless steel

2.3. Cleveland Flash Point and Fire Point Equipment. Frequency: 50 Hz, thermometer - 6°C to 400°C, voltage - 220 V,

Resolution: 0.1°C, Relative humidity - less than 85% RH, gross weight - about 6 Kg, Accuracy: 2°C

The flashpoint and fire point of petroleum products are determined using this apparatus (shown in Figure 3). Equipment consists of a cup, a heating plate with a swivel joint, and an energy regulator. Suitable for use on AC circuits with a voltage of 220 volts and a frequency of 50 cycles. Refer Table 1 for properties of oils.

2.4. Redwood Viscometer

Figure 6: Flow chart of the experimental procedure.

(i) Type of Bath: electrically heated immersion heater

(ii) Heater: tubular immersion heater

(iii) Input power supply: 230v AC, 50 Hz

(iv) Stirrer: a manual stirrer with a stirrer blade is used to keep the temperature consistent throughout the chamber as shown in figure 4

The smoke, flash, and fire point of soyabean oil is measured and is given in Table 2.

2.5. Kinematic Viscosity.

$$\text{Kinematic viscosity } (\nu) = C * t -, \quad (2)$$

where $C = 0.0026$ for $t = 34$ to 100 sec.$C = 0.00247$ for $t > 100$ sec.$B = 0.5$.

Tables 2 and 3 represent the kinematic viscosity of base oil and nanofluid, respectively.

2.6. Work Material Used. A nickel-based superalloy, Inconel 718 has features such as limited thermal conductivity, work hardening, and the ability to maintain strength in high-temperature environments, and it is tough to cut [37–40]. As a result, surface smoothness is critical when machining Inconel 718. The SEM and EDM spectrum of Inconel 718 material is shown in figure 5. Chemical composition of Inconel 718 is measured on an EDS machine available at Shivaji University, Kolhapur. It is mentioned in Table 4.

2.7. Experimentation. Initially round bar of Inconel 718 workpiece was clamped on a machine spindle using three jaw chuck and tool holder fixed into the hexagonal turret. All the experimental runs were performed randomly according to the L_{18} orthogonal array. A 30 mm cutting length is set for the experimental purpose and each experiment performed using fresh cutting edge.

To supply nanofluid in the cutting zone, MQL setup was used. However, MQL setup is having two inlet ports and one outlet port for oil mist. Out of the two inlet ports, one inlet port is for compressed air supply at fixed pressure, and nanofluid is supplied through another inlet port. Further, the compressed air supply and nanofluid are mixed together and supplied to the cutting zone through the nozzle. The flow rate of nanofluid is controlled by the knob which is available on the MQL setup.

Table 9: Experimental results of surface roughness and tool wear in μm.

Expt. no	Flow rate	Cutting speed	Weight %	Feed rate	Roughness	Tool Wear
1	80	92.99	1	0.1	3.100	0.18
2	80	92.99	2	0.2	2.338	0.20
3	80	92.99	3	0.3	1.900	0.22
4	80	104.61	1	0.1	3.729	0.25
5	80	104.61	2	0.2	2.672	0.23
6	80	104.61	3	0.3	2.101	0.26
7	80	116.23	1	0.2	4.394	0.36
8	80	116.23	2	0.3	3.772	0.37
9	80	116.23	3	0.1	2.375	0.35
10	160	92.99	1	0.3	2.503	0.21
11	160	92.99	2	0.1	1.733	0.18
12	160	92.99	3	0.2	1.203	0.17
13	160	104.61	1	0.2	3.186	0.39
14	160	104.61	2	0.3	2.177	0.36
15	160	104.61	3	0.1	1.515	0.32
16	160	116.23	1	0.3	3.732	0.50
17	160	116.23	2	0.1	2.597	0.48
18	160	116.23	3	0.2	2.038	0.47

Table 10: SN ratios of surface roughness and tool wear.

Ex. no.	S/N ratio for surface roughness	S/N ratio for tool wear
1	-9.8272	14.8945
2	-7.3769	13.9794
3	-5.5751	13.1515
4	-11.4318	12.0412
5	-8.5367	12.7654
6	-6.4485	11.7005
7	-12.8572	8.8739
8	-11.5314	8.6360
9	-7.5133	9.1186
10	-7.9692	13.5556
11	-4.7760	14.8945
12	-1.6053	15.3910
13	-10.0649	8.1787
14	-6.7572	8.8739
15	-3.6083	9.8970
16	-11.4388	6.0206
17	-8.2894	6.3752
18	-6.1841	6.5580

The MTAB control system is employed in the CNC machine for experimentation, and its additional specifications are listed in Table 5.

2.8. Design of Experiments. In Minitab V16 software, the experiment was designed using mixed-level Taguchi orthogonal array. The levels of the input variables selected based on the past literature were machine tool capacity and cutting tool manufacture data and initial experiment. Four parameters were assumed for design of experiments, namely, flow rate with 2 levels (80 and 160 ml/hr), cutting speed with 3 levels (92.99, 104.61, and 116.23 m/min), feed with 3 levels (0.1, 0.2, and 0.3 m/min), and weight % of nanoparticles with 3 levels (0.1, 0.2, and 0.3%). Table 6 lists the controlled parameters used during the experiment. Table 7 shows the constant parameters used during the experiment. Table 8 shows the orthogonal array.

As illustrated in Figure 6, a Mitutoyo tester model SJ-210 was used to measure surface roughness. After one machining, machined Inconel 718 bar's surface roughness was measured.

Specifications:

Speed: 0.5 millimetres per second.

Cut-off: 5 mm.

As shown in Figure 6, the Mitutoyo microscope is utilised to determine tool wear rate. This toolmaker's microscope has a least count of 0.005 mm.

3. Results and Discussion

The machined components were tested for output parameters. The output characteristics are tool wear and surface roughness investigated in this research. This section contains the acquired results. Minitab 17 software was used to analyze the experimental data, and two tests were run for each factor. Cutting speed, weight % of nanoparticles, flow rate, and feed were all examined.

After each cut, the tool inserts were removed from the tool holder and were inspected under the toolmaker's microscope for flank wear measurement. Finally, surface roughness was measured on machined surface using the portable surface roughness tester (Mitutoyo: model SJ-210). For surface roughness measurement, machined surface was clamped on the V block. Surface roughness was measured along the circumferential direction of machined surface at three specified locations. The average value of surface roughness was considered for analysis and the cut-off length of tester was 5 mm.

Experimental results of surface roughness and tool wear are shown in Table 9, and values of their SN Ratios are shown in Table 10.

3.1. ANOVA Approach for Determining Significant Process Parameters for Surface Roughness. x-Axis illustrates various levels of input variables, while y-Axis outlines the average S/N ratio. Figure 7 shows the main effect plot surface roughness S/N ratio. Figure 8 shows as the flow rate increases, the surface roughness diminishes. It stems from the fact that the number of nanoparticles increases at the tool-workpiece interface with increasing flow rate, which takes heat away from the cutting zone [41–45]. Rolling effect and deposition of CuO on worn surfaces leading to decrease frictional coefficient ultimately reduced surface roughness. Increase in feed rate, as well as speed, increases surface roughness. Surface roughness diminishes as the weight % of nanoparticles increases. As the nanoparticles'

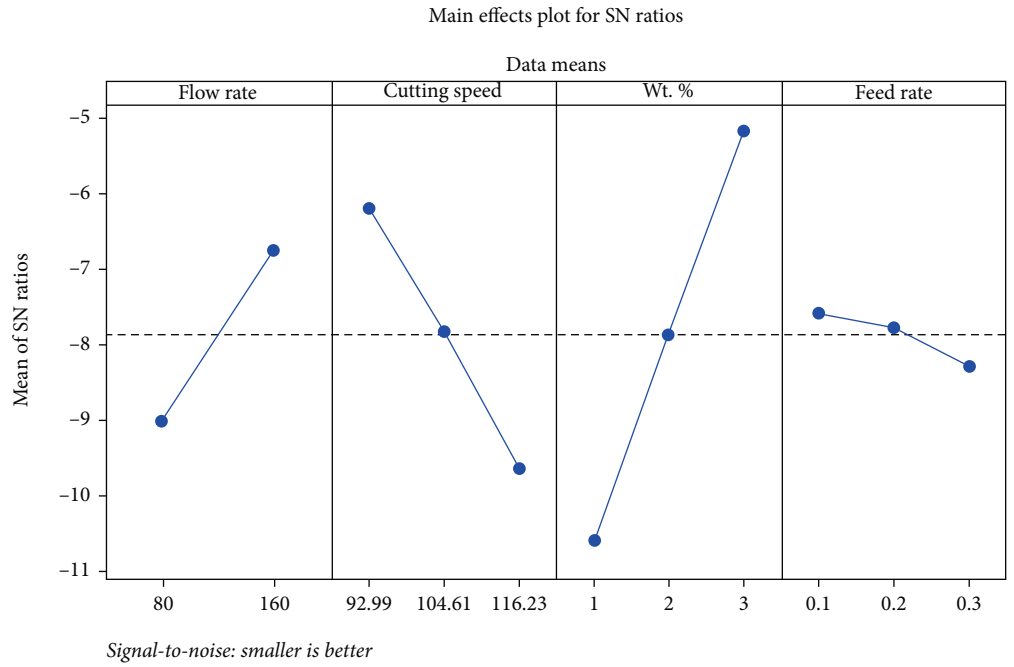

Figure 7: Main effect plot of S/N ratio for surface roughness.

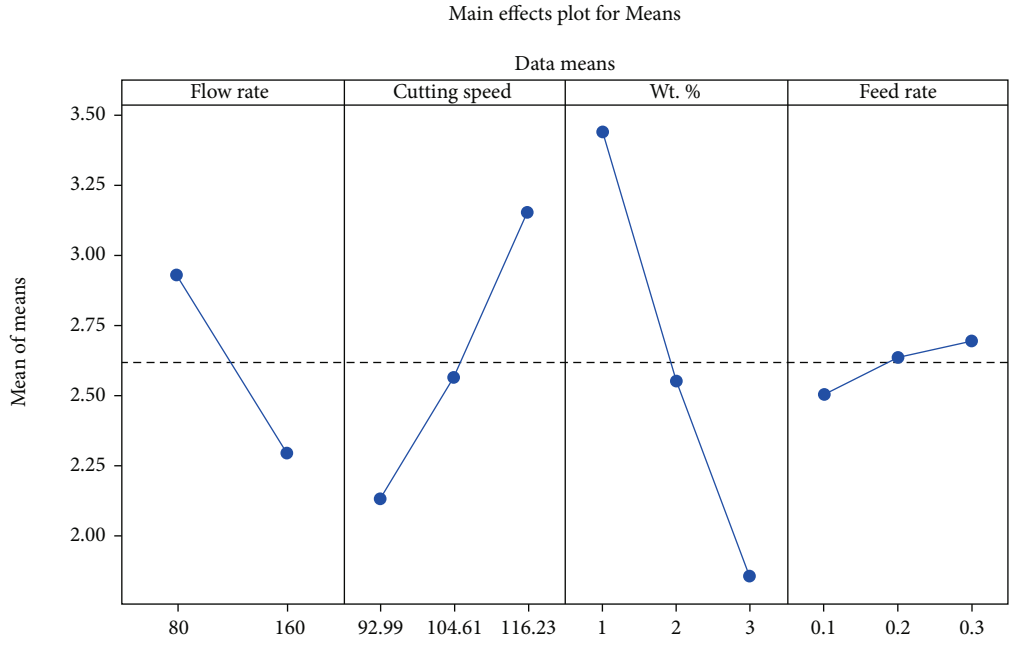

Figure 8: Main effect plot for means for surface roughness.

concentration in the base fluid rises, the number of nanoparticles at the tool-workpiece interface increases. As a result of functioning as a spacer between the tool and the workpiece, the contact between the two is minimized, and the surface roughness is reduced. Cutting speed has a significant impact on residual tensions. MQL may cause residual stresses at any cutting speed, resulting in increased surface roughness due to these residual stresses. This could be due to the slurry effect of MQL fluid. CuO nanoparticles have antiwear properties [46–49]. This is due to the rolling action and CuO deposition on worn surfaces, which results in a lower frictional coefficient. This rolling effect and spacer action is well illustrated in Figure 9.

Table 11 shows that the percentage contribution of flow rate to surface roughness is 24.97%, cutting speed is 21.83%,

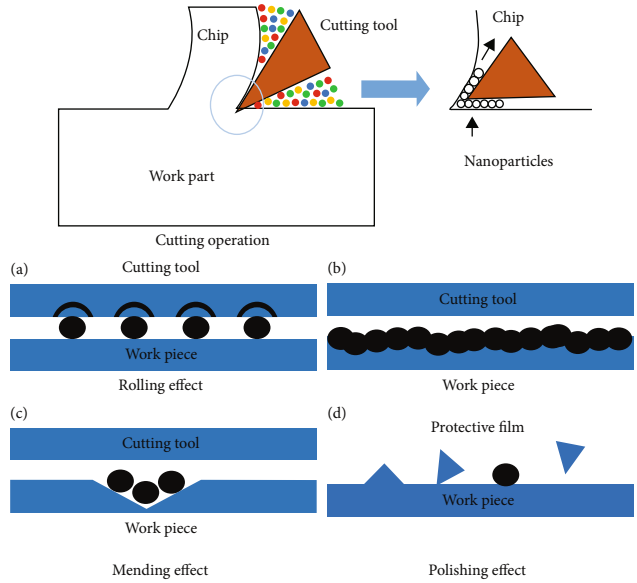

Figure 9: Possible lubrication mechanism.

Table 11: Analysis of variance for surface roughness.

Source	DF	Adj. SS	Adj. MS	*F* value	*P* value	% contribution
Flow rate	1	1.8031	1.80310	53.97	0.000	24.97
Cutting speed	2	3.1562	1.57810	47.23	0.000	21.83
Weight %	2	7.5797	3.78986	113.43	0.000	52.43
Feed	2	0.1126	0.05631	1.69	0.234	0.78
Error	10	0.3341	0.03341			
Total	17	12.9857				

Table 12: Response table for S/N Ratios for Ra value, Smaller is better.

Level	Flow rate	Cutting speed	Weight %	Feed rate
1	2.931	2.130	3.441	2.508
2	2.298	2.563	2.548	2.639
3		3.151	1.855	2.697
Delta	0.633	1.022	1.585	0.189
Rank	3	2	1	4

feed is 0.78%, and the weight % of nanoparticles is 52.43%. Cutting speed and nanoparticle weight % are the most important factors influencing surface roughness.

Table 12 shows the weight % of nanoparticles has the largest impact on surface roughness, subsequently cutting speed, flow rate, and feed. Nanoparticle quantum at tool-workpiece contact increases, as the concentration of nanoparticles in base fluid rises. As a result of a decrease in contact between workpiece and tool by acting as a spacer between tool and workpiece, surface roughness is reduced. Weight % of nanoparticles is a major influencing factor in residual stresses.

Viscosity of oil decreases with the increase in temperature. Temperature increases with the increase in cutting speed, and hence viscosity decreases. This decreased viscosity is not able to carry heat from cutting zone at high cutting speed, and hence at high cutting speed, because of reduced viscosity of nanofluid, surface roughness start decreasing. An increase in nanoparticle concentration in base fluid causes an increase in the number of nanoparticles at the interface of the tool and workpiece. This results in the decrease in contact between workpiece and tool by acting as a spacer between tool and workpiece, consequently surface roughness is reduced.

3.2. ANOVA Approach for Determining Significant Process Parameters for Tool Wear. *x*-Axis illustrates various input variable levels, while *y*-Axis outlines the average S/N ratio. Figure 10 shows the main effect plot for the tool wearing the S/N ratio. As flow rate, speed, and feed rate increase, tool wear increases; however, as weight % increases, tool wear decreases, as shown in Figure 11.

From Table 13, it can be observed that for tool wear percentage contribution of cutting speed is 75.24%, the flow rate is 23.27%, feed is 1.05%, and weight% is 0.425%. This implies tool wear is influenced by cutting speed.

Table 14 shows rankings based on delta statistics, where delta refers to the overall change in a value [50–52]. Delta is considered the difference between a start and end value, irrespective of fluctuations between these points that compare the relative magnitude of effects. The difference between the highest and the lowest average value among levels of a factor gives a delta statistic value. The higher the rank, the greater the influence of the control parameter on output characteristics. The ranks and delta values for various

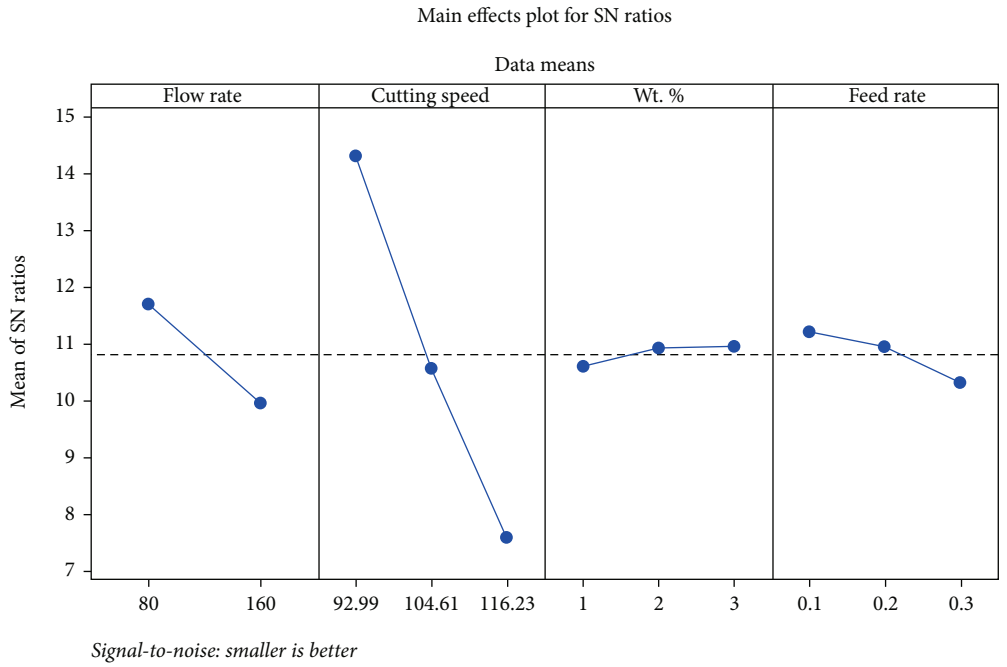

Figure 10: Main effect plot of S/N ratio for tool wear.

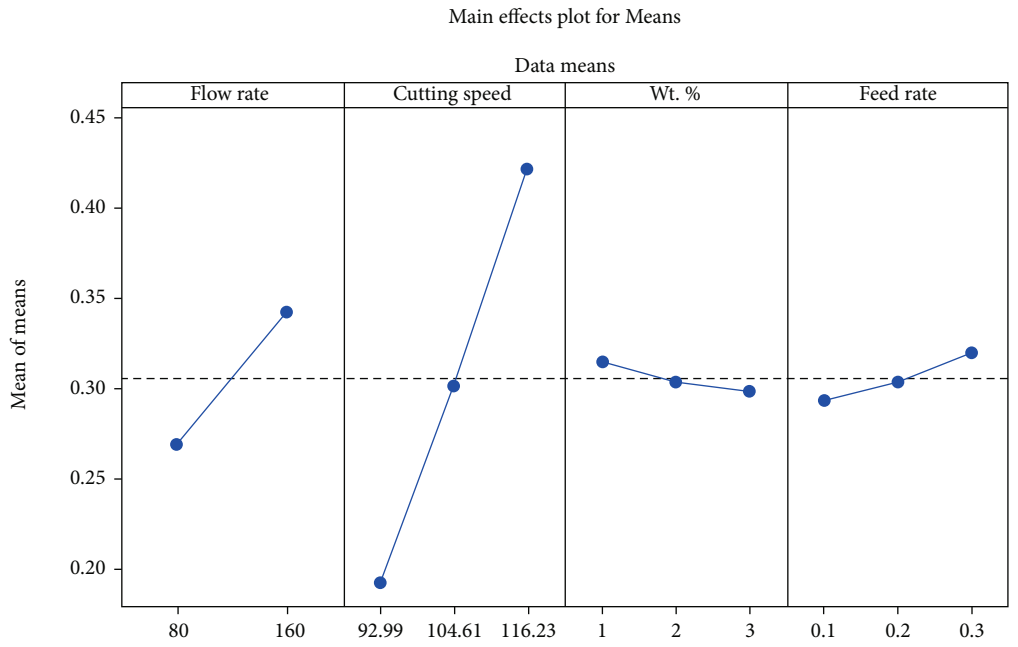

Figure 11: Main effect plot for means for tool wear.

Table 13: Analysis of variance for tool wear.

Source	DF	Adj. SS	Adj. MS	*F* value	*P* value	% contribution
Flow rate	1	0.0242	0.0242	12.58	0.005	23.27
Cutting speed	2	0.156544	0.078272	40.67	0.000	75.24
Weight%	2	0.000878	0.000439	0.23	0.8	0.425
Feed	2	0.002178	0.001089	0.57	0.585	1.05
Error	10	0.019244	0.001924			
Total	17	0.203044				

Table 14: Confirmation experiments for surface roughness and tool wear.

	Optimum levels	Prediction by Taguchi method	Experiment
Surface roughness	Flow rate: 160 ml/hr, Cutting speed: 92.99 m/min, Weight % of CuO: 3, Feed rate: 0.1 mm/min.	1.26	1.102
Tool Wear	Flow rate: 80 ml/hr, Cutting speed: 92.99 m/min, weight % of CuO: 3, Feed rate: 0.1 mm/min.	0.164	0.15

Table 15: Response table for S/N Ratios for tool wear smaller is better.

Level	Flow rate	Cutting speed	Weight %	Feed rate
1	0.2689	0.1933	0.3150	0.2933
2	0.3422	0.3017	0.3033	0.3033
3		0.4217	0.2983	0.3200
Delta	0.0733	0.2283	0.0167	0.0267
Rank	2	1	4	3

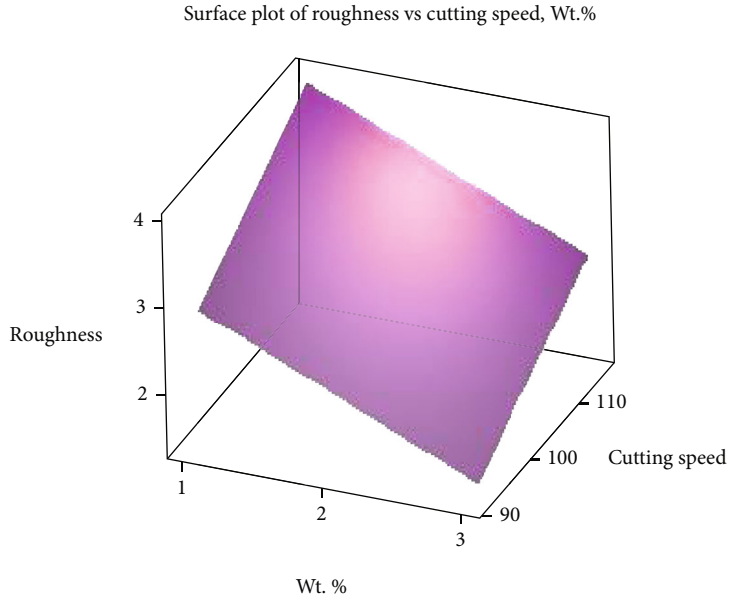

Figure 12: Response surface for surface roughness vs. cutting speed, weight %.

parameters show that speed has the greatest effect on tool wear subsequently flow rate, feed rate, and weight%.

This may be because as cutting speed increases, higher temperature gets associated with the tool and correlated effect of temperature on wear characteristics of the tool. Increasing temperature leads to the decrease in viscosity, and hence heat carried way at the tool tip reduces with increasing cutting speed. With the increase in the weight % of CuO decreases the cutting force gradually, but this reduction rate of cutting force was lowered down with increasing weight % of nanoparticles. This may be due to higher percentages of particle agglomerate. Good tribological properties and cooling properties of CuO particles lead to less tool wear. This may be because with increasing air pressure, the flow rate increases, leading to the formation of small droplets of aerosol from oil, and its size decreases with increasing the air pressure. These small size aerosols that easily enter into the tool-cheap interface cause removal of heat and consequently less tool wear.

3.3. Predicted Result by Taguchi Method. Once the optimal level of the geometry parameters is identified, the final

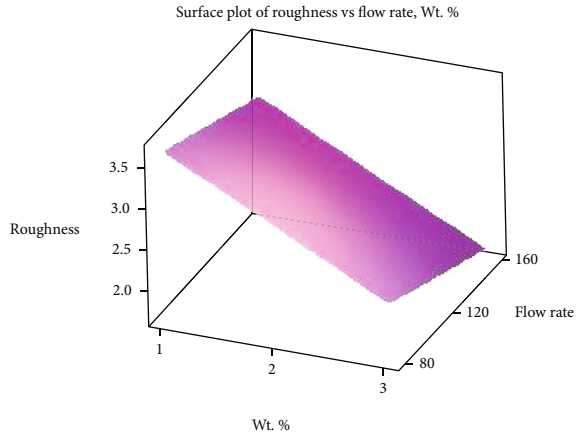

Figure 13: Response surface for surface roughness vs. flow rate, weight %.

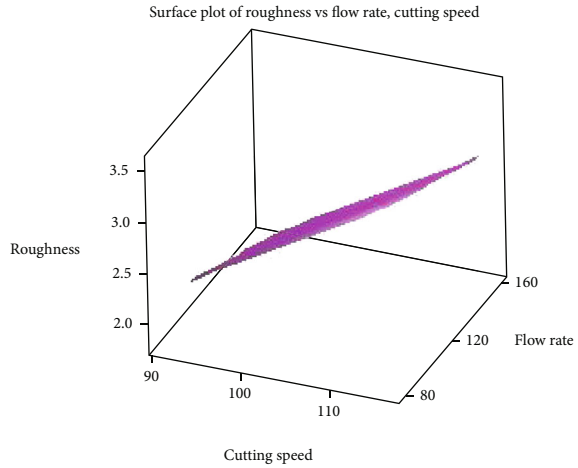

Figure 14: Response surface for surface roughness vs. cutting speed, flow rate.

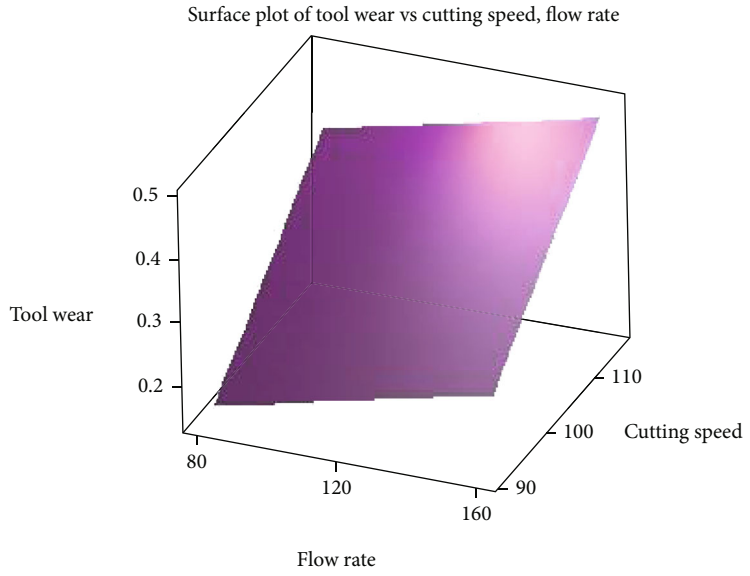

Figure 15: Response surface for tool wear vs. cutting speed, flow rate.

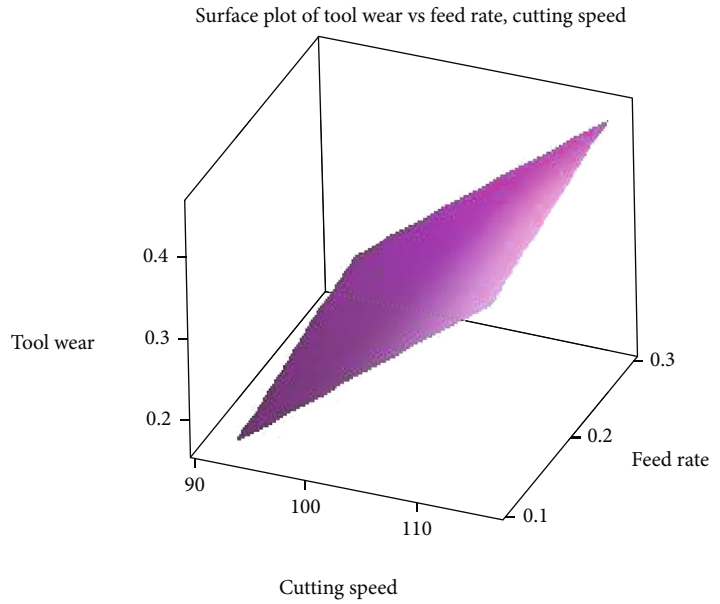

Figure 16: Response surface for tool wear vs. cutting speed, feed rate.

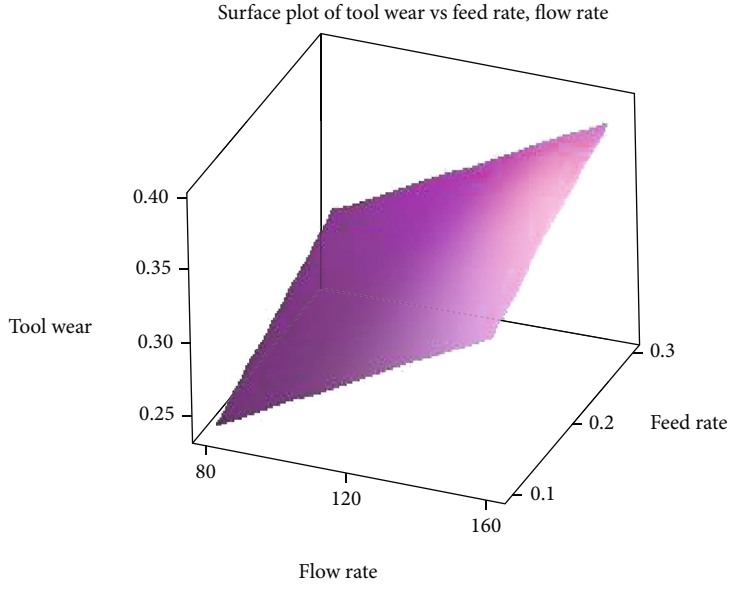

Figure 17: Response surface for tool wear vs. flow rate, feed rate.

step is to predict and validate the improvement of the performance measures using the optimal level, i.e., for surface roughness flow rate is 160 ml/hr, cutting speed is 92.99 m/min, weight % of CuO is 3, and feed rate is 0.1 mm/min, and for tool wear flow rate is 80 ml/hr, cutting speed is 92.99 m/min, weight % of CuO is 3, and feed rate is 0.1 mm/min. The purpose of the confirmation experiment is to verify the conclusions drawn during the analysis phase. The S/N ratio η_{pre} for tensile strength can be predicted as follows:

$$\eta_{\text{pre}} = \eta_{\text{om}} + (\eta_{\text{flowrate}} - \eta_{\text{om}}) + \left(\eta_{\text{cutting speed}} - \eta_{\text{om}}\right) + \left(\eta_{\text{weight\%}} - \eta_{\text{om}}\right) + (\eta_{\text{feed rate}} - \eta_{\text{om}}), \tag{3}$$

where ηom is the overall mean S/N ratio and $\eta_{flowrate}$ $\eta cutting_{speed}$,$\eta_{weight\%}$, and $\eta_{feed\,rate}$ are the S/N ratios of the significant individual control factors at their optimum levels.

The optimum S/N ratio for surface roughness: from Table 11,

$$\begin{aligned}\eta_{\text{om}} &= -7.8773,\\ \eta\text{flow}_{\text{rate}} &= -6.7436,\\ \eta_{\text{cutting speed}} &= -6.1883,\\ \eta_{\text{weight\%}} &= -5.1558,\\ \eta_{\text{feed rate}} &= -7.5743.\end{aligned} \tag{4}$$

Putting these values we get

$$\eta_{\text{pre}} = -2.0301. \tag{5}$$

Predicted optimum surface roughness is

$$\sqrt{10^{-\eta_{opt}/10}} = 1.26. \tag{6}$$

3.4. The Optimum S/N Ratio for Tool Wear. From Table 11,

$$\begin{aligned}\eta_{\text{om}} &= 10.8281,\\ \eta_{\text{flow rate}} &= 11.7,\\ \eta_{\text{cutting speed}} &= 14.3110,\\ \eta_{\text{weight\%}} &= 10.9694,\\ \eta_{\text{feed rate}} &= 11.2035.\end{aligned} \tag{7}$$

Putting these values we get

$$\eta_{\text{pre}} = 15.6843. \tag{8}$$

Predicted optimum tool wear is

$$\sqrt{10^{-\eta_{opt}/10}} = 0.164. \tag{9}$$

When optimal levels of input parameters are determined, then the next stage is to forecast and validate the improvement of performance measures with the help of the optimal level. Below are the recommended levels for output parameters.

(a) For surface roughness: flow rate: 160 ml/hr, cutting speed: 92.99 m/min, weight % of CuO: 3, and feed rate: 0.1 mm/min

(b) For Tool wear: flow rate: 80 ml/hr, cutting speed: 92.99 m/min, weight % of CuO: 3, and feed rate: 0.1 mm/min

3.5. Regression Method. To find out the correlation between factors, response surface regression was performed using the software Minitab 17. From eighteen experiments, observed responses, i.e., surface roughness and tool wear, were used to compute the model. The response was correlated with the factors using the first-order polynomial. The relationship between surface roughness, tool wear, and process parameters for first-order response surface model is developed using RSM as mentioned in Table 15.

The mathematical model for surface roughness and tool wear are

$$\begin{aligned}&\text{Surface roughness} = 0.361 - 0.00791 * \text{Flow rate} + 0.04397 * \text{Cutting Speed} - 0.7927 * \text{Weight\%} + 0.947 * \text{Feed rate},\\ &\text{Tool wear} = -0.842 + 0.000917 * \text{Flow rate} + 0.009825 * \text{Cutting Speed} - 0.0083 * \text{Weight\%} + 0.133 * \text{Feed rate}.\end{aligned} \tag{10}$$

For this model R^2 value for surface roughness = 96.90%, R^2(adj.) = 95.94% and R^2 value for tool wear = 90.41%, R^2 (adj.) = 87.46% this indicate that the model is desirable and 96.90% and 90.41% variability is explained by the model after considering significant parameters for surface roughness and tool wear, respectively.

For above-fitted model, response surfaces are shown in the following figures.

3.6. Effect of Cutting Speed and Weight % on Surface Roughness. The contour plot shown in Figure 12 indicates that the lowest roughness is obtained when weight % is high and cutting speed is low [31–33]. This area appears at the front right corner of the plot. In addition, we can see the shape of the response surface and get a general idea of surface roughness at various settings of cutting speed and weight %.

The contour plot shown in Figure 13 indicates that the lowest roughness is obtained when weight % and cutting speed are high [34–37]. This area appears at the back right corner of the plot. In addition, we can see the shape of the response surface and get a general idea of surface roughness at various settings of flow rate and weight %.

The contour plot shown in Figure 14 indicates that the lowest roughness is obtained when the flow rate is high and cutting speed is low [38–40]. This area appears at the back left corner of the plot. In addition, we can see the shape of the response surface and get a general idea of surface roughness at various settings of flow rate and cutting speed.

The contour plot in Figure 15 indicates that the lowest tool wear is obtained when the flow rate is low and cutting speed is low. This area appears at the front left corner of the plot. In addition, we can see the shape of the response surface and get a general idea of tool wear at various settings of flow rate and cutting speed.

The contour plot in Figure 16 indicates that the lowest tool wear is obtained with a low feed rate and cutting speed. This area appears at the front left corner of the plot. In addition, we can see the shape of the response surface and get a general idea of tool wear at various settings of feed rate and cutting speed.

The contour plot in Figure 17 indicates that the lowest tool wear is obtained with low feed and flow rates. This area appears at the front left corner of the plot. In addition, we can see the shape of the response surface and get a general idea of tool wear at various settings of feed rate and flow rate.

Validation of experiment was conducted by considering optimal values of input process parameters as follows:

(1) For Surface roughness: 160 ml/hr flow rate, 92.99 m/min cutting speed, 3 weight % of CuO, and 0.1 mm/min feed rate, and for tool wear they are

(2) For tool wear: 80 ml/hr flow rate, 92.99 m/min cutting speed, 3 weight % of CuO, and 0.1 mm/min feed rate

Experiments are conducted by using these optimal levels for each parameter. Results obtained from validation experimentation are shown in Table 14. It compares the predicted and actual responses obtained during the experimental trial. The predicated and actually measured responses for surface roughness and tool wear are in good agreement, indicating that optimization of the control parameters is appropriate.

4. Conclusion

In this experimental study the effect of cutting parameters on machinability aspect were analysed to improve the machining performance in terms of the tool wear and surface roughness. Based on the experimental results and statistical analysis following conclusions are drawn.

(1) CuO nanoparticles are equally distributed in soyabean oil using a magnetic stirrer and an ultrasonic bath compared to sunflower oil and distilled water without clumping together

(2) Weight %, cutting speed, and flow rate are the significant factors that have impact on surface roughness, and of each contributing 52.43%, 21.83%, and 24.97%, respectively. Surface roughness is reduced by the rolling effect and thin film layer of soyabean oil with CuO nanoparticle in machining zone, which helps to reduce the coefficient of friction

(3) Higher tool wear rate was observed in case of high cutting speed due to generation of high temperature in machining zone which reduces viscosity of nanofluid and hence ultimately decreases base oil capacity to carry heat. Further, cutting speed is the highest influencing factor for the tool wear

(4) The optimal value of surface roughness was observed at the combination of 160 ml/hr flow rate, 92.99 m/min cutting speed, 3 weight % of CuO, and 0.1 mm/min feed rate using the Taguchi method

(5) Predicted optimal values of the process parameters for tool wear are 80 ml/hr flow rate, 92.99 m/min cutting speed, 3 weight % of CuO, and 0.1 mm/min feed rate by the Taguchi method

Data Availability

The data available is based on the reasonable request to corresponding author.

Conflicts of Interest

The authors declare that they have no conflicts of interest.

Acknowledgments

The authors extend their appreciation to the Deanship of Scientific Research at King Khalid University (KKU) for funding this research through the Research Group Program under the grant number: (R.G.P.2/248/43). The author B. Saleh is grateful to the Taif University Researchers Supporting Project number (TURSP-2020/49), Taif University, Taif, Saudi Arabia for the financial support.

References

[1] Y. S. Dambatta, A. A. D. Sarhan, M. B. A. K. Sayuti, and M. H. B. A. Shukor, "Fuzzy logic method to investigate grinding of alumina ceramic using minimum quantity lubrication," *International Journal of Applied Ceramic Technology*, vol. 16, no. 4, pp. 1668–1683, 2019.

[2] V. S. Sharma, G. Singh, and K. Sorby, "A review on minimum quantity lubrication for machining processes," *Materials and Manufacturing Processes*, vol. 30, no. 8, pp. 935–953, 2015.

[3] N. M. Tuan, T. M. Duc, V. L. Hoang, and T. B. Ngoc, "Investigation of Machining Performance of MQL and MQCL Hard Turning Using Nano Cutting Fluids," *Fluids*, vol. 7, no. 5, p. 143, 2022.

[4] M. A. Makhesana, K. M. Patel, and N. Khanna, "Analysis of vegetable oil-based nano-lubricant technique for improving machinability of Inconel 690," *Journal of Manufacturing Processes*, vol. 77, pp. 708–721, 2022.

[5] H. Hegab and H. Kishawy, "Towards sustainable machining of Inconel 718 using nano-fluid minimum quantity lubrication," *Journal of Manufacturing and Materials Processing*, vol. 2, no. 3, p. 50, 2018.

[6] R. Rosnan, M. N. Murad, A. I. Azmi, and I. Shyha, "Effects of minimal quantity lubricants reinforced with nano-particles on the performance of carbide drills for drilling nickel-titanium alloys," *Tribology International*, vol. 136, pp. 58–66, 2019.

[7] Y. Shokoohi, E. Khosrojerdi, and B. H. Rassolian Shiadhi, "Machining and ecological effects of a new developed cutting fluid in combination with different cooling techniques on turning operation," *Journal of Cleaner Production*, vol. 94, pp. 330–339, 2015.

[8] R. Bag, A. Panda, A. K. Sahoo, and R. Kumar, "A brief study on effects of nano cutting fluids in hard turning of AISI 4340 steel," *Materials Today: Proceedings*, vol. 26, pp. 3094–3099, 2020.

[9] H. Hegab and H. A. Kishawy, "Machining of Inconel 718 using nano-fluid minimum quantity lubrication," in *7th International Conference on Virtual Machining Process Technology (VMPT) 2018*, Hamilton, Canada, May 7-9, 2018.

[10] H. Hegab, *Machining of Inconel 718 using nano-fluid minimum quantity lubrication*, Elsevier, 2019, No. May 2018.

[11] R. Padmini, P. Vamsi Krishna, and K. M. Rao, "Experimental evaluation of nano-molybdenum disulphide and nano-boric acid suspensions in vegetable oils as prospective cutting fluids during turning of AISI 1040 steel," *Proceedings of the Institution of Mechanical Engineers, Part J: Journal of Engineering Tribology*, vol. 230, no. 5, pp. 493–505, 2016.

[12] F. Pashmforoush and R. Delir Bagherinia, "Influence of water-based copper nanofluid on wheel loading and surface roughness during grinding of Inconel 738 superalloy," *Journal of Cleaner Production*, vol. 178, pp. 363–372, 2018.

[13] Ş. Şirin and T. Kıvak, "Performances of different eco-friendly nanofluid lubricants in the milling of Inconel X-750 superalloy," *Tribology International*, vol. 137, pp. 180–192, 2019.

[14] K. Venkatesan, S. Devendiran, and N. M. Ghazaly, "Application of Taguchi-response surface analysis to optimize the cutting parameters on turning of Inconel X-750 using nanofluids suspended Al_2O_3 in coconut oil," *Procedia Manufacturing*, vol. 30, pp. 90–97, 2019.

[15] H. Hegab, U. Umer, M. Soliman, and H. A. Kishawy, "Effects of nano-cutting fluids on tool performance and chip morphology during machining Inconel 718," *International Journal of Advanced Manufacturing Technology*, vol. 96, no. 9–12, pp. 3449–3458, 2018.

[16] H. Hegab, B. Darras, and H. A. Kishawy, "Sustainability assessment of machining with nano-cutting fluids," *Procedia Manufacturing*, vol. 26, pp. 245–254, 2018.

[17] H. A. Kishawy, H. Hegab, I. Deiab, and A. Eltaggaz, "Sustainability assessment during machining Ti-6Al-4V with nano-additives-based minimum quantity lubrication," *Journal of Manufacturing and Materials Processing*, vol. 3, no. 3, p. 61, 2019.

[18] A. Eltaggaz and I. Deiab, "The Effect Of Nanoparticle Concentration On Mql Performance When Machining Ti-6Al-4V Titanium Alloy," in *Progress in Canadian Mechanical Engineering*, York University, May 2018.

[19] M. Amrita, R. R. Srikant, A. V. Sitaramaraju, M. M. S. Prasad, and P. V. Krishna, "Experimental investigations on influence of mist cooling using nanofluids on machining parameters in turning AISI 1040 steel," *Proceedings of the Institution of Mechanical Engineers, Part J: Journal of Engineering Tribology*, vol. 227, no. 12, pp. 1334–1346, 2013.

[20] K. D. Vázquez, D. S. Cantú, A. F. Segura, F. Araiz, L. Peña-Parás, and D. Maldonado, "Application of nanofluids to improve tool life in machining processes," in *Proceedings of the LUBMAT*, pp. 1–8, Manchester, UK, 2014, no. *Paper number*: L146058.

[21] N. K. Mani, C. Mathew, and P. M. Kallanickal, "Optimization of cutting parameters & nanoparticle concentration in CNC turning of EN8 steel using Al2O3 nanofluids as coolant," *International Journal of Engineering Trends and Technology (IJETT)*, vol. 29, no. 6, pp. 290–294, 2015.

[22] M. M. Prasad and R. R. Srikant, "Performance evaluation of nano graphite inclusions in cutting fluids with Mql technique in turning of Aisi 1040 steel," *International Journal of Research in Engineering and Technology*, vol. 2, no. 11, pp. 381–393, 2013.

[23] M. Usha and G. S. Rao, "Optimization of multiple objectives by genetic algorithm for turning of AISI 1040 steel using Al_2O_3 nano fluid with MQL," *Tribology in Industry*, vol. 42, no. 1, pp. 70–80, 2020.

[24] A. Thakur, A. Manna, and S. Samir, "Multi-response optimization of turning parameters during machining of EN-24 steel with SiC Nanofluids based minimum quantity lubrication," *Silicon*, vol. 12, no. 1, pp. 71–85, 2020.

[25] M. A. Mahboob Ali, A. I. Azmi, A. N. Mohd Khalil, and K. W. Leong, "Experimental study on minimal nanolubrication with surfactant in the turning of titanium alloys," *International Journal of Advanced Manufacturing Technology*, vol. 92, no. 1–4, pp. 117–127, 2017.

[26] N. M. M. Reddy and P. K. Chaganti, "Investigating optimum SiO2 nanolubrication during turning of AISI 420 SS," *Engineering, Technology & Applied Science Research*, vol. 9, no. 1, pp. 3822–3825, 2019.

[27] K. Venkatesan, A. T. Mathew, S. Devendiran, N. M. Ghazaly, S. Sanjith, and R. Raghul, "Machinability study and multi-response optimization of cutting force, surface roughness and tool wear on CNC turned Inconel 617 superalloy using Al_2O_3 nanofluids in coconut oil," *Procedia Manufacturing*, vol. 30, pp. 396–403, 2019.

[28] H. Hegab, A. Salem, S. Rahnamayan, and H. A. Kishawy, "Analysis, modeling, and multi-objective optimization of machining Inconel 718 with nano-additives based minimum quantity coolant," *Applied Soft Computing*, vol. 108, p. 107416, 2021.

[29] K. Venkatesan, S. Devendiran, K. Nishanth Purusotham, and V. S. Praveen, "Study of machinability performance of Hastelloy-X for nanofluids, dry with coated tools," *Materials and Manufacturing Processes*, vol. 35, no. 7, pp. 751–761, 2020.

[30] K. V. Ramanan, S. Ramesh Babu, M. Jebaraj, and K. Nimel Sworna Ross, "Face turning of Incoloy 800 under MQL and nano MQL environments," *Materials And Manufacturing Processes*, vol. 36, no. 15, pp. 1769–1780, 2021.

[31] K. Camali, R. Demirsoz, M. Boy, M. Korkmaz, and N. Yasar, "Performance of MQL and nano-MQL lubrication in machining ER7 steel for train wheel applications," *Lubricants*, vol. 10, no. 4, p. 48, 2022.

[32] M. Korkmaz, M. Gupta, M. Boy, N. Yasar, and G. Krolczyk, "Influence of duplex jets MQL and nano-MQL cooling system on machining performance of Nimonic 80A," *Journal of Manufacturing Processes*, vol. 69, pp. 112–124, 2021.

[33] A. Afzal, C. A. Saleel, S. Bhattacharyya, N. S. Olusegun, and D. Samuel, "Merits and limitations of mathematical modeling and computational simulations in mitigation of COVID -19 pandemic: a comprehensive review," *Archives of Computational Methods in Engineering*, vol. 29, pp. 1311–1337, 2022.

[34] A. Belhocine and A. Afzal, "Computational finite element analysis of brake disc rotors employing different materials,"

Australian Journal of Mechanical Engineering, vol. 20, no. 3, pp. 637–650, 2022.

[35] Z. Arshad, A. H. Khoja, S. Shakir et al., "Magnesium doped TiO_2 as an efficient electron transport layer in perovskite solar cells," *Thermal Engineering*, vol. 26, article 101101, 2021.

[36] M. S. Ali, Z. Anwar, M. A. Mujtaba et al., "Two-phase frictional pressure drop with pure refrigerants in vertical mini/micro-channels. Case study," *Thermal Engineering*, vol. 23, article 100824, 2021.

[37] N. Akram, E. Montazer, S. N. Kazi et al., "Experimental investigations of the performance of a flat-plate solar collector using carbon and metal oxides based nanofluids," *Energy*, vol. 227, p. 120452, 2021.

[38] M. A. Mujtaba, H. Muk Cho, H. H. Masjuki et al., "Effect of primary and secondary alcohols as oxygenated additives on the performance and emission characteristics of diesel engine," *Energy Reports*, vol. 7, pp. 1116–1124, 2021.

[39] M. El, H. Attia, Z. Driss et al., "Phosphate bed as energy storage materials for augmentation of conventional solar still productivity," *Environmental Progress & Sustainable Energy*, vol. 40, no. 4, 2021.

[40] A. R. Kaladgi, A. Afzal, A. D. Mohammad Samee, and M. K. Ramis, "Investigation of dimensionless parameters and geometry effects on heat-transfer characteristics of liquid sodium flowing over a flat plate," *Heat Transfer—Asian Research*, vol. 48, no. 1, pp. 62–79, 2019.

[41] Z. Ansari, A. R. Faizabadi, and A. Afzal, "Fuzzy C-least medians clustering for discovery of web access patterns from web user sessions data," *Intelligent Data Analysis*, vol. 21, no. 3, pp. 553–575, 2017.

[42] S. P. Wategave, N. R. Banapurmath, M. S. Sawant et al., "Clean combustion and emissions strategy using reactivity controlled compression ignition (RCCI) mode engine powered with CNG-Karanja biodiesel," *Journal of the Taiwan Institute of Chemical Engineers*, vol. 124, pp. 116–131, 2021.

[43] A. Afzal, A. D. M. Samee, R. K. A. Razak, and M. K. Ramis, "Thermal management of modern electric vehicle battery systems (MEVBS)," *Journal of Thermal Analysis and Calorimetry*, vol. 144, no. 4, pp. 1271–1285, 2021.

[44] I. Mokashi, A. Afzal, S. A. Khan et al., "Nusselt number analysis from a battery pack cooled by different fluids and multiple back-propagation modelling using feed-forward networks," *International Journal of Thermal Sciences*, vol. 161, article 106738, 2021.

[45] M. E. M. Soudagar, M. A. Kalam, M. U. Sajid et al., "Thermal analyses of minichannels and use of mathematical and numerical models," *Numerical Heat Transfer, Part A: Applications*, vol. 77, no. 5, pp. 497–537, 2020.

[46] A. Afzal, A. D. M. Samee, R. K. A. Razak, and M. K. Ramis, "Heat transfer characteristics of MWCNT nanofluid in rectangular mini channels," *International Journal of Heat and Technology*, vol. 36, no. 1, pp. 222–228, 2018.

[47] A. Afzal, A. D. Mohammed Samee, A. Javad, S. Ahamed Shafvan, P. V. Ajinas, and K. M. Ahammedul Kabeer, "Heat transfer analysis of plain and dimpled tubes with different spacings," *Heat Transfer Research*, vol. 47, no. 3, pp. 556–568, 2018.

[48] O. Ziaee, N. Zolfaghari, M. Baghani, M. Baniassadi, and K. Wang, "A modified cellular automaton model for simulating ion dynamics in a li-ion battery electrode," *Energy Equipment and Systems*, vol. 10, no. 1, pp. 41–49, 2022.

[49] M. S. Taslimi, S. Maleki Dastjerdi, S. Bashiri Mousavi, P. Ahmadi, and M. Ashjaee, "Assessment and multi-objective optimization of an off-grid solar based energy system for a Conex," *Energy Equipment and Systems*, vol. 9, no. 2, pp. 127–143, 2021.

[50] M. Sharifi, M. Amidpour, and S. Mollaei, "Investigating carbon emission abatement long-term plan with the aim of energy system modeling; case study of Iran," *Energy Equipment and Systems*, vol. 6, no. 4, pp. 337–349, 2018.

[51] S. Sabzi, M. Asadi, and H. Moghbelli, "Review, analysis and simulation of different structures for hybrid electrical energy storages," *Energy Equipment and Systems*, vol. 5, no. 2, pp. 115–129, 2017.

[52] M. Hadad, J. Gholampour Darzi, A. Mahdianikhotbesara, and J. Makarian, "Experimental investigation of the effect of single point dressing parameters on grinding of Mo40 hardened steel using mounted point grinding tool," *Energy Equipment and Systems*, vol. 10, no. 2, pp. 197–214, 2022.